Interior Transition Layers in Flight-Path Optimization

Mark D. Ardema*
Santa Clara University, Santa Clara, California
and
L. Yang†
Sterling Software, Palo Alto, California

Interior transition layers occur in flight path optimization by singular perturbation methods whenever the reduced solution exhibits multiple branches. Although such phenomena occur in many problems, it has been little studied in the literature. In this paper, we consider interior transition layers in vertical-plane climb path optimization. Our approach is to treat the interior layer associated with the transonic energy state discontinuity as two boundary layers, one in forward time and the other in backward time. The initial states of the two boundary layers are matched to give continuous composite solutions at the point of reduced solution discontinuity.

Introduction

CONDITIONS under which a singularly perturbed optimal control problem may be formally decomposed into three subproblems—an initial boundary-layer problem, an outer problem, and a terminal boundary-layer problem—are discussed in Refs. 1 and 2. These reduced-order systems may then be solved asymptotically and combined to obtain a uniformly valid asymptotic representation of the original system by a method such as matched asymptotic expansions.[3]

One of the conditions required for this decoupling is the existence of a continuous solution of the reduced problem. It has been found, however, that the application of singular perturbation methods to flight-path optimization frequently results in problems with discontinuous reduced solutions. A well-known example is the vertical-plane optimal climb problem, when posed so that energy E is the single slow state variable.[4,5] In this case, the reduced solution is the energy climb path, which is discontinuous for "low-performance" aircraft (i.e., aircraft with relatively low transonic values of thrust-drag/weight).[6,7] Reduced solution discontinuities also occur when altitude h and velocity V are modeled as slow state variables.[8,9]

A more striking example of reduced solution discontinuity is found in three-dimensional energy state extremals. In this case, discontinuities are the rule rather than the exception and, in fact, multiple discontinuities are typical.[10] Thus, the ability to deal with discontinuities in the reduced solution is crucial to asymptotic analysis of flight-path optimization, particularly in three dimensions.

In reduced-order approximations, discontinuities require instantaneous jumps in the fast variables, similar to the jumps required at the boundaries. And, just as at the boundaries, these jumps imply the need to introduce boundary-layer-type transitions to arrive at uniformly valid approximations; we call these *interior transition layers*. It is clear that if n is the number of discontinuities in the reduced solution, then the singularly perturbed optimal control problem must be decomposed into $3+2n$ reduced-order subproblems, each of which is to be solved asymptotically and matched with its neighbors.

Despite their importance, there has been only limited investigation of interior layers. Breakwell[8,9] has studied transitions in vertical-plane aircraft climb problems under the assumption that drag D does not depend on lift L. In effect, this uncouples the state equations and results in a singularly perturbed system with h and V as slow state variables and flight path angle γ as fast, if $D/L_{\max}$ (or a multiple) is used as a small parameter. Because of the simplicity of the fast subsystem in this formulation, Breakwell is able to accomplish a rather complete asymptotic analysis of the various transition layers.

A more popular singularly perturbed dynamic model of the climb path problem is the energy state model obtained by substituting E for V as a state variable and then treating E as slow and h and γ as fast. This has the advantages that the outer, or reduced, solution is the well-known energy climb path and the coupling between h and γ is not neglected.[11] The fast subsystem of equations, however, is now fourth order (in h, γ, and their corresponding adjoints) and must be solved numerically as a two-point boundary-value problem. The only rigorous investigation of interior layers for this formulation has been that of Weston et al.[7] In their approach, the solution of the interior layer equations is sought such that the weighted sum of the squares of the errors between the initial and final conditions and the corresponding reduced solution values is a minimum. Thus, the cost functional contains eight arbitrary parameters (two for each state and adjoint variable) that must be prespecified. The transition time and the transition location must also be prespecified, bringing to 10 the number of parameters that must be selected a priori. Finally, to complete our survey of past work, Refs. 12 and 13 adopt ad hoc engineering approaches to interior layers in vertical plane climb problems.

In this paper, we study interior transitions in the two-dimensional energy state model, but with an approach different from that in Weston et al.[7] Our approach is to treat the interior layer as two boundary layers with free initial states, one in forward and one in backward time. The initial states of the two boundary layers are then matched at the discontinuity, giving a continuous transition across the reduced solution discontinuity.

Problem Formulation and Energy Climb Path

We begin with the usual singularly perturbed equations of motion of the vertical-plane, point-mass, energy-state dynamic model,[5,7]

Presented as Paper 86-2037 at the AIAA Guidance, Navigation and Control Conference, Williamsburg, VA, Aug. 18–20, 1986; received Sept. 15, 1986; revision received March 3, 1987.

*Professor and Chairman, Department of Mechanical Engineering (formerly with NASA Ames Research Center). Associate Fellow AIAA.

†Staff Analyst.

$$\dot{E} = P$$
$$\epsilon\dot{h} = V\sin\gamma$$
$$\epsilon\dot{\gamma} = g(n - \cos\gamma)/V \tag{1}$$

where

$$P(E,h,n) = V(T - D)/W$$
$$V(E,h) = \sqrt{2g(E-h)}$$
$$n = L/W$$
$$D(E,h,n) = A + Bn^2 \tag{2}$$

where $T(E,h)$, $A(E,h)$, and $B(E,h)$ are given functions. It is desired to minimize the time-to-climb, t_f, between two specified state points;

$$E(0) = E_i \qquad E(t_f) = E_f$$
$$h(0) = h_i \qquad h(t_f) = h_f$$
$$\gamma(0) = \gamma_i \qquad \gamma(t_f) = \gamma_f \tag{3}$$

The single control variable is the load factor n.

Applying the maximum principle for singularly perturbed systems[3] gives the necessary conditions for optimal control as[5,7]

$$\dot{\lambda}_E = -\lambda_E P_E - \frac{g\lambda_h}{V}\sin\gamma + \frac{g^2\lambda_\gamma}{V^3}(n - \cos\gamma)$$
$$\epsilon\dot{\lambda}_h = -\lambda_E P_h + \frac{g\lambda_h}{V}\sin\gamma - \frac{g^2\lambda_\gamma}{V^3}(n - \cos\gamma) \tag{4}$$
$$\epsilon\dot{\lambda}_\gamma = -\lambda_h V\cos\gamma - \frac{g\lambda_\gamma}{V}\sin\gamma$$

$$n = \frac{gW\lambda_\gamma}{2V^2B\lambda_E} \tag{5}$$

$$H = -1 + \lambda_E P + \lambda_h V\sin\gamma + \frac{g\lambda_\gamma}{V}(n - \cos\gamma) = 0 \tag{6}$$

where

$$P_E = \partial P/\partial E \quad \text{and} \quad P_h = \partial P/\partial h.$$

Setting $\epsilon = 0$ in Eqs. (3–6) gives the reduced solution[5]

$$\gamma_r = 0, \qquad n_r = 1, \qquad P_{h_r} = 0$$
$$\lambda_{h_r} = 0, \qquad \lambda_{E_r} = \frac{1}{P_r}, \qquad \lambda_{\gamma_r} = \frac{2V_r^2 B_r}{gWP_r} \tag{7}$$

For some aircraft, $P_{h_r} = 0$ has multiple roots, indicating multiple local maxima of $P(E,h,n)$ with E and n fixed (Fig. 1). Since h plays the role of a control variable in the reduced problem, it is clear that it is the global maximum of P that is of interest, i.e.,

$$h_r = \arg\max_h P(E,h,n)\Big|_{\substack{E=\text{const}\\ n=1}} \tag{8}$$

This defines a path in the (V,h) plane, the well-known energy climb path.[4–7] If for some energy $\bar{E}$ there are two equal relative local maxima, and for $E < \bar{E}$ the higher one gives the global maximum whereas for $E > \bar{E}$ the lower one gives the global maximum (Fig. 1), then the energy climb path will be discontinuous at $\bar{E}$ (solid line in Fig. 2). We note that all control and fast state variables may be discontinuous at a discontinuity of the reduced solution; however, for our problem only h_r and λ_{γ_r} are discontinuous, whereas E_r, γ_r, λ_{E_r}, λ_{h_r}, and n_r are all continuous.

Interior Layer Analysis

Nonlinear Equations

It is well known that the reduced solution of singularly perturbed systems provides a locus of equilibrium points for boundary-layer equations and that these equilibrium points are saddles of type m (where m is the number of fast state variables).[3,5,7,14–16] Therefore, a direct integration of the interior layer equations across a discontinuity of the reduced solution will not, in general, be possible because it would involve a two-point boundary-value problem between two unstable equilibrium points.

To avoid this difficulty, we treat the interior layer as the composition of two boundary layers—a forward and a backward layer—both beginning at time $t = \bar{t}$, where $\bar{t}$ is the time at $\bar{E}$ on the reduced solution. To this end, we introduce the stretched time variables,

$$t_1 = (\bar{t} - t)/\epsilon, \qquad t_2 = (t - \bar{t})/\epsilon \tag{9}$$

Substituting Eq. (9) into Eqs. (1) and (4) and then setting $\epsilon = 0$, the zero-order boundary-layer equations are

$$(-1)^i\frac{dh_i}{dt_i} = V_i\sin\gamma_i \qquad (-1)^i\frac{d\gamma_i}{dt_i} = \frac{g(n_i - \cos\gamma_i)}{V_i}$$
$$(-1)^i\frac{d\lambda_{h_i}}{dt_i} = -\bar{\lambda}_E P_{h_i} + \frac{g\lambda_{h_i}}{V_i}\sin\gamma_i - \frac{g^2\lambda_{\gamma_i}}{V_i^3}(n_i - \cos\gamma_i)$$
$$(-1)^i\frac{d\lambda_{\gamma_i}}{dt_i} = -\lambda_{h_i}V_i\cos\gamma_i - \frac{g\lambda_{\gamma_i}}{V_i}\sin\gamma_i \tag{10}$$

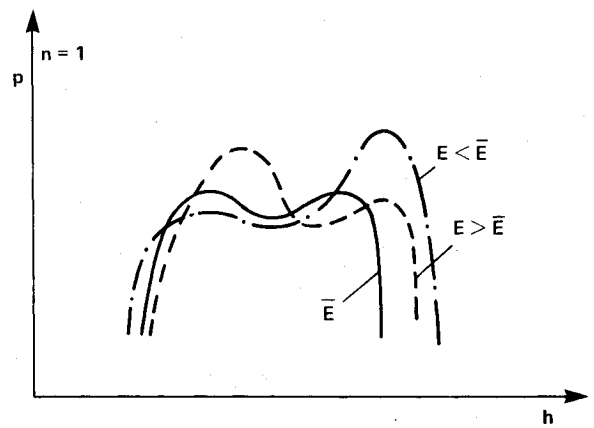

Fig. 1 Variation of $P(E,h,n)$ with h at various values of E.

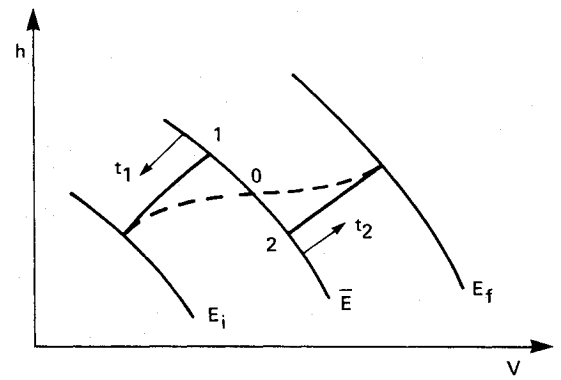

Fig. 2 Reduced (energy state) solution in the (h,V) plane.

for $i=1,2$, where $V_i=\sqrt{2g(\bar{E}-h_i)}$. The point labeled 1 on Fig. 2 is the equilibrium point for the backward boundary layer ($i=1$) and point 2 is the equilibrium point for the forward boundary layer ($i=2$). Equations (5) and (6) become

$$n_i=\frac{gW\lambda\gamma_i}{2V_i^2B_i\bar{\lambda}_E} \tag{11}$$

$$H_i=-1+\bar{\lambda}_EP_i+\lambda_{h_i}V_i\sin\gamma_i+\frac{g\lambda\gamma_i}{V_i}(n_i-\cos\gamma_i)=0 \tag{12}$$

Next we take up the issue of selection of initial conditions for the boundary-layer equations (10). Noting that the transition will consist of a push-over followed by a pull-up, the load factor history will be as shown in Fig. 3, where it is assumed that the transition from push-over to pull-up occurs precisely at $\bar{E}$. The appropriate conditions are then: 1) $h_{0_i}=h_i(0)$ preselected; 2) $n_{0_i}=1$; 3) $H_{0_i}=0$; and 4) instability suppressed. More explicitly, using Eqs. (2), (7), (11), and (12), these conditions may be written as

$$h_{0_i}\text{ preselected}$$

$$\lambda\gamma_{0_i}=2V_{0_i}^2B_{0_i}/gW\bar{P}$$

$$\lambda_{h_{0_i}}=\frac{1-\dfrac{P_{0_i}+2V_{0_i}B_{0_i}(1-\cos\gamma_{0_i})/W}{\bar{P}}}{V_{0_i}\sin\gamma_{0_i}}$$

$$\gamma_{0_i}\text{ selected to suppress instability} \tag{13}$$

where the quantities with overbars refer to equilibrium values and where $\bar{P}=\bar{P}_1=\bar{P}_2=1/\bar{\lambda}_E$. Thus, in terms of Ref. 14, we have a boundary-layer problem of type B.

Solving the backward ($i=1$) boundary-value problem [Eqs. (10–13)] for various values of h_{0_1}, $\bar{h}_2\le h_{0_1}\le\bar{h}_1$, generates a function $\gamma_{0_1}(h_{0_1})$; similarly, repetitive solution of the forward ($i=2$) problem gives $\gamma_{0_2}(h_{0_2})$. The specific solutions of interest are then those for which $\gamma_{0_1}=\gamma_{0_2}=\gamma_0$ and $h_{0_1}=h_{0_2}=h_0$, provided such solutions exist. These solutions, when joined together, give continuity of all variables and their derivatives at $t=\bar{t}$. Assuming the initial and terminal boundary layers are asymptotically negligible at the transition layer, locally uniformly valid approximations may be formed by additive composition in the usual way.[3] Recalling that $\epsilon=1$,

$$h_a(t)=h_r(t)+\left\{\begin{matrix}h_1(\bar{t}-t)-\bar{h}_1,\ 0\le t\le\bar{t}\\ h_2(t-\bar{t})-\bar{h}_2,\ \bar{t}<t\le t_f\end{matrix}\right\}$$

$$\gamma_a(t)=\left\{\begin{matrix}\gamma_1(\bar{t}-t),\ 0\le t\le\bar{t}\\ \gamma_2(t-\bar{t}),\ \bar{t}<t\le t_f\end{matrix}\right\}$$

$$\lambda_{h_a}(t)=\left\{\begin{matrix}\lambda_{h_1}(\bar{t}-t),\ 0\le t\le\bar{t}\\ \lambda_{h_2}(t-\bar{t}),\ \bar{t}<t\le t_f\end{matrix}\right\}$$

$$\lambda\gamma_a(t)=\frac{2V_r^2(t)B_r(t)}{gWP_r(t)}+\left\{\begin{matrix}\lambda\gamma_1(\bar{t}-t)\\ -\dfrac{2\bar{V}_1^2\bar{B}_1}{gW\bar{P}},\ 0\le t\le\bar{t}\\ \lambda\gamma_2(t-\bar{t})\\ -\dfrac{2\bar{V}_2^2\bar{B}_2}{gW\bar{P}},\ \bar{t}<t\le t_f\end{matrix}\right\}$$

$$n_a(t)=\left\{\begin{matrix}n_1(\bar{t}-t),\ 0\le t\le\bar{t}\\ n_2(t-\bar{t}),\ \bar{t}<t\le t_f\end{matrix}\right\} \tag{14}$$

These functions give a trajectory passing through point h_0 at time $\bar{t}$ as shown by the dashed line in Fig. 2; they are all continuous, but not necessarily differentiable, at $\bar{t}$.

Linear Equations

After the manner of Ref. 14, we now linearize the forward and backward transition layer equations about their equilibrium points. The solutions to these equations, which will be obtained in algebraic form, have two possible uses. First, the linear solutions give qualitative insights into the behavior of the transition layer equations, particularly in regard to their stability properties. Second, if the jump in the reduced solution at time $\bar{t}$ is relatively small, the linear solutions may provide an adequate quantitative approximation.

We first write the transition layer variables as the sum of their equilibrium values and small perturbations,

$$h_i(t_i)=\bar{h}_i+\alpha_i(t_i)$$

$$\gamma_i(t_i)=\beta_i(t_i)$$

$$\lambda_{h_i}(t_i)=\theta_i(t_i)$$

$$\lambda\gamma_i(t_i)=\frac{2\bar{V}_i^2\bar{B}_i}{gW\bar{P}}+\delta_i(t_i)$$

$$n_i(t_i)=1+\eta_i(t_i)$$

$$i=1,2 \tag{15}$$

Substituting these expressions into Eq. (10) and retaining only first-order terms in the perturbation variables gives a fourth-order linear system with two stable and two unstable modes.

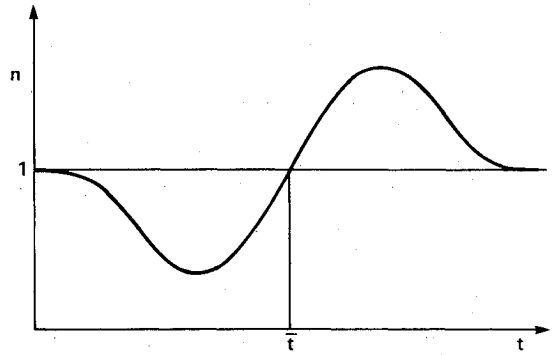

Fig. 3 Load factor time history.

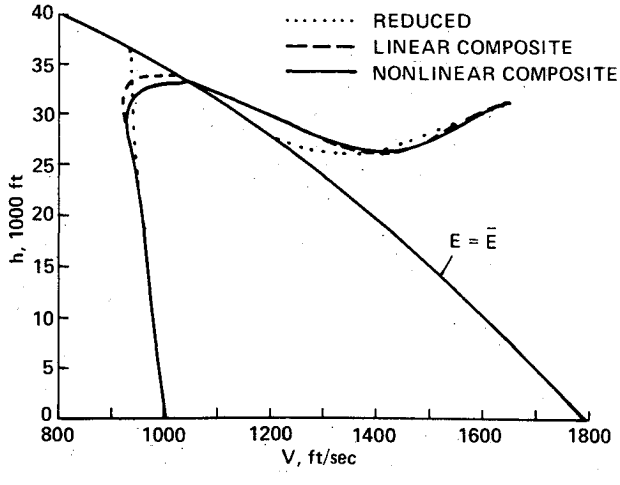

Fig. 4 Reduced and composite solutions in the flight envelope.

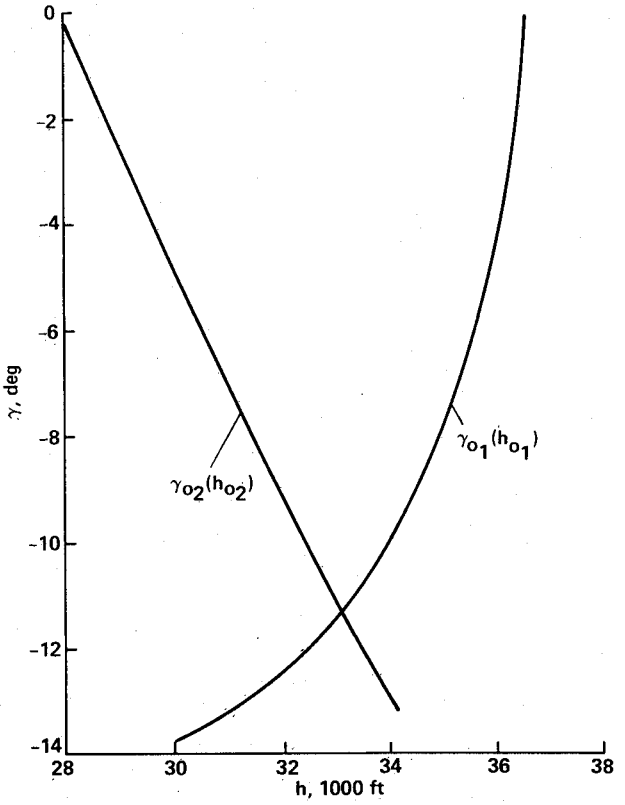

Fig. 5 Boundary-layer initial condition functions.

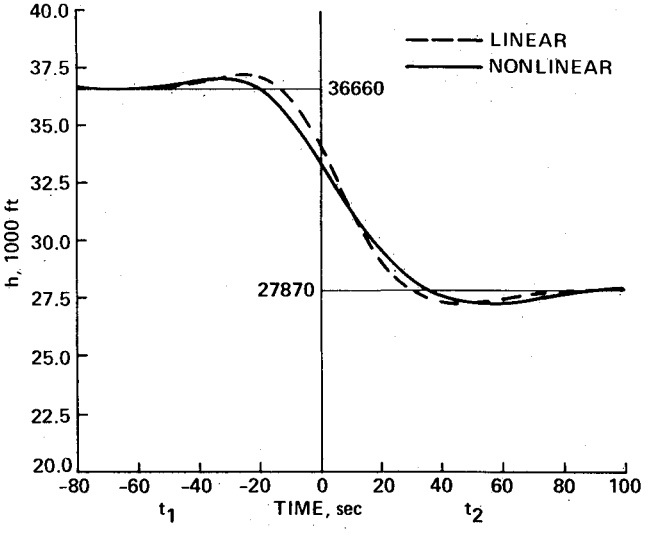

Fig. 6 Altitude time history.

The initial conditions for these equations are

$$\alpha_i(0) = h_0 - \bar{h}_i$$

$$\delta_i(0) = \frac{2V_0^2 B_0}{g\bar{W}\bar{P}} - \frac{2\bar{V}_i^2 \bar{B}_i}{g\bar{W}\bar{P}}$$

$$\left.\begin{matrix}\beta_i(0)\\ \theta_i(0)\end{matrix}\right\} \text{ selected to suppress unstable modes} \qquad (16)$$

With the aid of Ref. 14, the solution to this linear initial-value

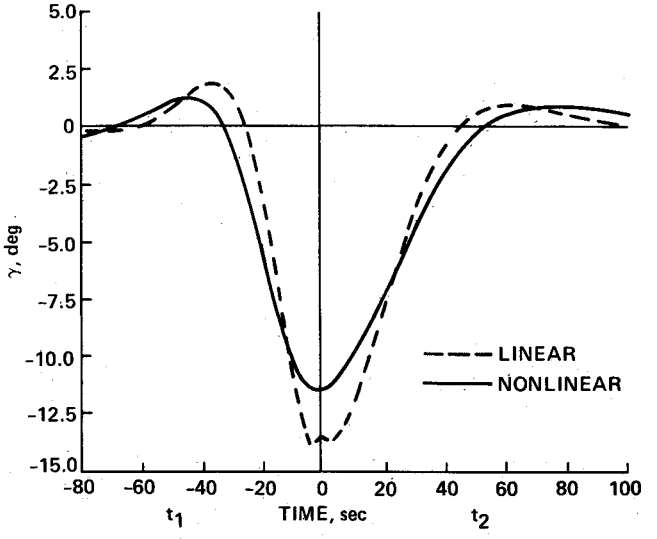

Fig. 7 Flight path angle time history.

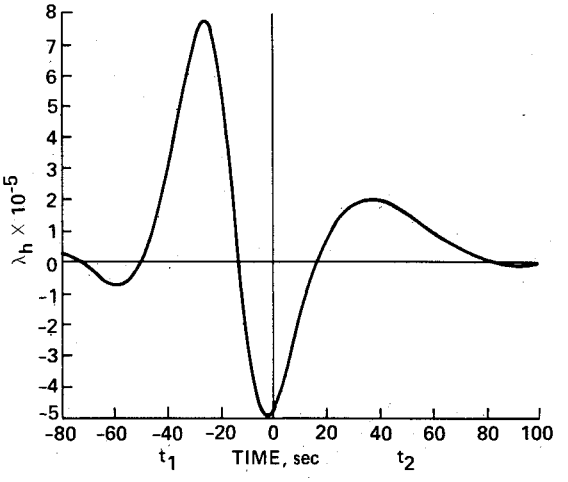

Fig. 8 Altitude adjoint time history.

problem for the altitude and flight path perturbations is

$$\alpha_1(t_1) = \frac{(h_0 - \bar{h}_1)e^{-a_1 t_1}}{2a_1 b_1} \times \left[2a_1 b_1 \cos(b_1 t_1) + (K_1 + a_1^2 - b_1^2)\sin(b_1 t_1)\right]$$

$$\alpha_2(t_2) = \frac{(h_0 - \bar{h}_2)e^{-a_2 t_2}}{2a_2 b_2} \times \left[2a_2 b_2 \cos(b_2 t_2) + (K_2 + a_2^2 - b_2^2)\sin(b_2 t_2)\right]$$

$$\beta_1(t_1) = -\frac{(h_0 - \bar{h}_1)e^{-a_1 t_1}}{2\bar{V}_1}\left[\frac{1}{a_1}(K_1 - a_1^2 - b_1^2)\cos(b_1 t_1) + \frac{1}{b_1}(-K_1 - a_1^2 - b_1^2)\sin(b_1 t_1)\right]$$

$$\beta_2(t_2) = \frac{(h_0 - \bar{h}_2)e^{-a_2 t_2}}{2\bar{V}_2}\left[\frac{1}{a_2}(K_2 - a_2^2 - b_2^2)\cos(b_2 t_2) + \frac{1}{b_2}(-K_2 - a_2^2 - b_2^2)\sin(b_2 t_2)\right] \qquad (17)$$

where

$$K_i = g\frac{\bar{V}_i^2\bar{B}_i - V_0^2 B_0}{\bar{V}_i^2\bar{B}_i(h_0 - \bar{h}_i)} + \frac{g\bar{B}_{h_i}}{\bar{B}_i} - \frac{2g^2}{\bar{V}_i^2} \tag{18}$$

and where a_i and b_i are the absolute values of the real and imaginary parts, respectively, of any (and of all) roots of

$$S_i^4 + \left(\frac{2g\bar{B}_{h_i}}{\bar{B}_i} - \frac{3g^2}{\bar{V}_i^2}\right)S_i^2 - \frac{g^2\bar{P}_{hh_i}W}{2\bar{V}_i\bar{B}_i} = 0 \tag{19}$$

To obtain h_0 and γ_0, we set $\beta_1(0) = \beta_2(0)$ in Eq. (17) and obtain

$$a_1\bar{V}_1(h_0 - \bar{h}_2)(K_2 - a_2^2 - b_2^2) = -a_2\bar{V}_2(h_0 - \bar{h}_1)(K_1 - a_1^2 - b_1^2) \tag{20}$$

Since $K_i(h_0)$ from Eq. (18), this is an implicit equation for h_0. The value of γ_0 is then determined from

$$\gamma_0 = \beta_1(0) = \beta_2(0) = \frac{(h_0 - \bar{h}_2)(K_2 - a_2^2 - b_2^2)}{2a_2\bar{V}_2} \tag{21}$$

The linear solution will be generally continuous, but not differentiable, at $t = \bar{t}$.

Numerical Example

Transition layer calculations were performed for a version of the F-4 aircraft. As shown in Fig. 4, the reduced solution (energy-state) of the path optimization problem has a discontinuity at an energy $\bar{E}$ of 49,940 ft, where altitude jumps from 36,660 to 27,870 ft. Forward and backward boundary-layer solutions were computed starting at initial conditions along $E = \bar{E}$, thereby generating the functions $\gamma_{0_1}(h_{0_1})$ and $\gamma_{0_2}(h_{0_2})$ as shown in Fig. 5. The point ($h_0 = 33{,}200$ ft, $\gamma_0 = -11.5$ deg) gives continuity of h and γ across the transition layer; these values are used in all the nonlinear calculations that follow.

Figures 6–10 show the time histories of the state, adjoint, and control variables of the nonlinear solution across the transition layer. As can be seen, these solutions make a smooth transition between the two branches of the reduced solution. The maneuver is very mild, the flight path reaching a

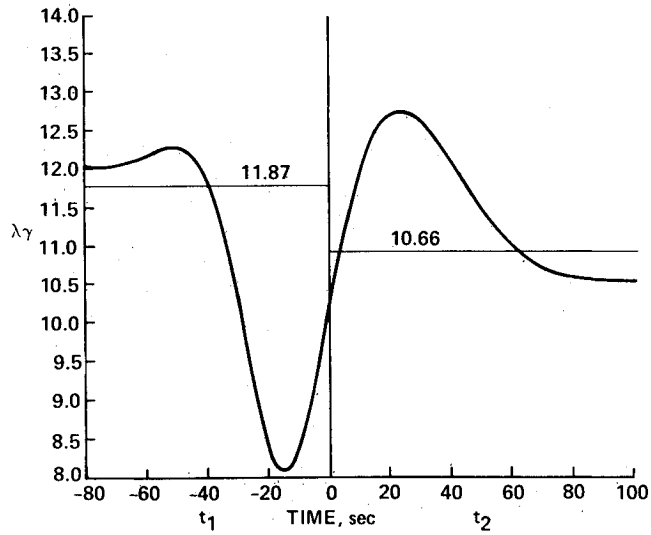

Fig. 9 Flight path adjoint time history.

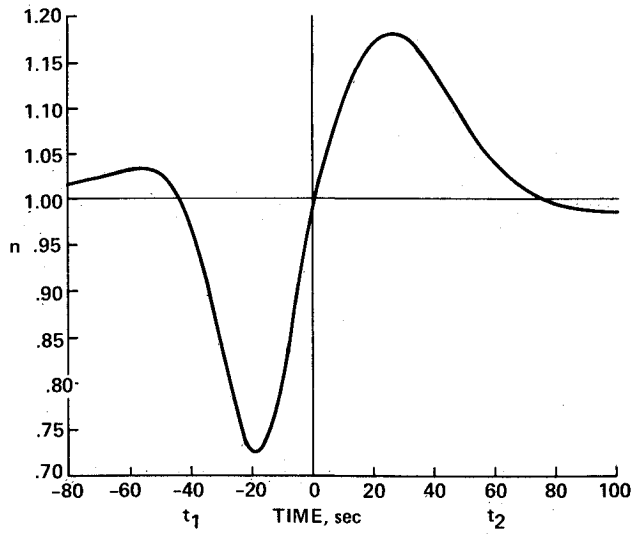

Fig. 10 Load factory time history.

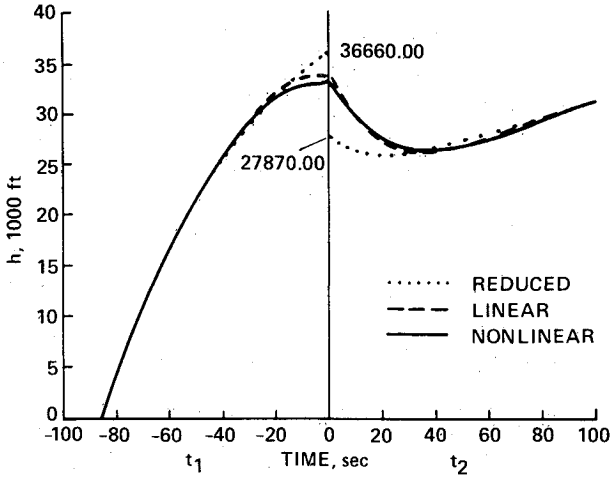

Fig. 11 Altitude composite solution.

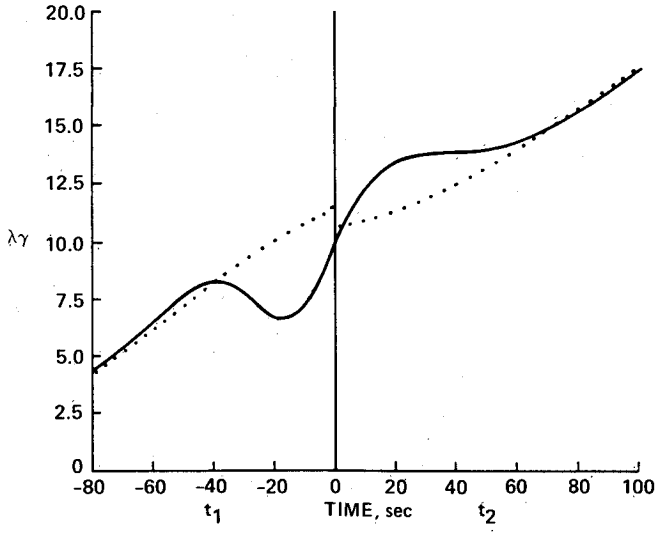

Fig. 12 Flight path adjoint composite solution.

minimum of only −11.5 deg and the maximum of the absolute value of the load factor deviation was only about 0.275. Also shown in Figs. 6 and 7 is the solution to the linearized equations. It appears that the linear solution provides a reasonable approximation to the nonlinear, although the former exhibits a discontinuity in the flight path angle time derivative at $\bar{E}$.

Next, we form the composite solutions according to Eq. (14) for the two variables that jump at $\bar{E}$, namely h and $\lambda\gamma$ (Figs. 11 and 12). Finally, both the nonlinear and linear paths are shown in the flight envelope plane in Fig. 4.

Conclusions

A useful method of open-loop analysis of interior transition layers occurring in flight path optimization has been developed. The method is based on treating the transition layer as two boundary layers matched at the point of reduced solution discontinuity. Application to a vertical plane climb problem showed that the transition maneuver was relatively benign in terms of deviations from reduced solution values of load factor and flight path angle.

References

[1]Freedman, M.I. and Kaplan, J.L., "Singular Perturbations of Two-point Boundary Value Problems Arising in Optimal Control," *SIAM Journal Control and Optimization*, Vol. 14, No. 2, Feb. 1976.

[2]Freedman, M.I. and Granoff, B., "Formal Asymptotic Solution of a Singularly Perturbed Nonlinear Optimal Control Problem," *Journal Optimization Theory and Applications*, Vol. 19, No. 2, June 1976.

[3]Ardema, M.D., "An Introduction to Singular Perturbations in Nonlinear Optimal Control," *Singular Perturbations in Systems and Control: CISM Courses and Lectures*, No. 280, edited by M.D. Ardema, International Center for Mechanical Sciences, Udine, Italy, 1983.

[4]Ardema, M.D., "Singular Perturbations in Flight Mechanics," NASA TM X-62,380, Aug. 1974 (revised July 1977).

[5]Ardema, M.D., "Solution of the Minimum Time-to-Climb Problem by Matched Asymptotic Expansions," *AIAA Journal*, Vol. 14, No. 7, July 1979.

[6]Bryson, A.E. Jr., Desai, M.N., and Hoffman, W.C., "Energy-State Approximation in Performance Optimization of Supersonic Aircraft," *Journal of Aircraft*, Vol. 6, Nov.–Dec. 1969.

[7]Weston, A.R., Cliff, E.M., and Kelley, H.J., "Altitude Transitions in Energy Climbs," *Automatica*, Vol. 19, Feb. 1983.

[8]Breakwell, J.V., "Optimal Flight-Path-Angle Transitions in Minimum-Time Airplane Climbs," *Journal of Aircraft*, Vol. 14, 1977.

[9]Breakwell, J.V., "More About Flight-Path-Angle Transitions in Optimal Airplane Climbs," *Journal of Guidance and Control*, Vol. 1, May–June 1978.

[10]Rajan, N. and Ardema, M.D., "Interception in Three Dimensions: An Energy Formulation," *Journal of Guidance, Control, and Dynamics*, Vol. 8, Jan.–Feb. 1985.

[11]Kelley, H.J., "Comments on 'A New Boundary-Layer-Matching Procedure for Singularly Perturbed Systems'," *IEEE Transactions on Automatic Control*, Vol. AC-23, No. 3, June 1978.

[12]Shinar, J. and Fainstein, V., "Improved Feedback Algorithms for Optimal Maneuvers in Vertical Plane," AIAA Paper 85-1976, 1985.

[13]Huynh, H.T. and Moreigne, O., "Quasi-Optimal On-Line Guidance Laws for Military Aircraft," AIAA Paper 85-1977, 1985.

[14]Ardema, M.D., "Linearization of the Boundary-Layer Equations of the Minimum Time-to-Climb Problem," *Journal of Guidance and Control*, Vol. 2, Sept.–Oct. 1979.

[15]Ardema, M.D., "Characteristics of the Boundary-Layer Equations of the Minimum Time-to-Climb Problem," *Proceedings of Fourteenth Annual Allerton Conference on Circuit and System Theory*, Allerton, Ill., 1976.

[16]Ardema, M.D. and Yang, L., "Picard Iterations of Boundary-Layer Equations," AIAA Paper 85-1964, 1985.